Radiation-hardened x-ray imaging for burning-plasma tokamaks

Fredrick H. Séguin
Boston Physics, 28 Commonwealth Avenue, Boston, Massachusetts 02116

Richard D. Petrasso and Chi Kang Li
Plasma Fusion Center, Massachusetts Institute of Technology, Cambridge, Massachusetts 012139

(Presented on 15 May 1996)

A special type of vacuum-photodiode detector is being developed for x-ray imaging of plasma in fusion-producing tokamaks such as the international thermonuclear experimental reactor (ITER), where the radiation environment will be too hostile for conventional x-ray detectors. The vacuum photodiode has modest efficiency, but it is intrinsically immune to radiation damage if built in such a manner as to expose only metal components to radiation. A design based on appropriately chosen materials (including high-Z cathodes) and geometries (including a small angle between cathode surface and incident x rays) can provide good signals from the 1–100 keV x rays that are of particular importance for imaging the plasmas in the Joint European Torus (JET) and ITER. It should also provide better rejection of signal distortion and noise due to unwanted detection of neutrons and hard gamma rays than conventional detectors. A prototype design is described, along with performance parameters predicted for JET and ITER. In addition, we show results of laboratory experiments that confirm some of the predicted behaviors of the design. © *1997 American Institute of Physics.* [S0034-6748(97)60801-1]

I. INTRODUCTION

X-ray imaging diagnostics provide crucial information about many tokamak plasma phenomena such as magneto-hydronamic (MHD) fluctuations and precursors to disruptive instabilities. But new detector technology is required for x-ray imaging on burning-plasma tokamaks such as the international thermonuclear experimental reactor (ITER), because the x-ray detectors used on existing tokamaks will fail quickly with exposure to the large fluxes of neutrons that characterize the harsh environment of the reactor tokamak (as observed[1] on the tokamak fusion test reactor TFTR during D-T operation). Operating with a fusion power output of 1000 MW, ITER would produce about 4×10^{20} n/s. Even with perfect shielding against indirect neutrons, silicon-based detectors would start to suffer radiation damage after only a few minutes in this environment (as will be discussed in Sec. IV).

In a search for a truly reliable detector design to use in imaging systems for this application, we start with the assumption that our detector must utilize only materials that are intrinsically immune to radiation damage. Vacuum photodiodes are simple and robust detectors that can satisfy this requirement easily, since they can be built almost entirely of metal. They have been used[2,3] for detecting ultraviolet and ultrasoft x-ray photons from tokamak plasmas, but we will show in the following sections how a special design can be optimized for detection of 1–100 keV x rays from ITER and from the Joint European Torus (JET).

II. VACUUM PHOTODIODE CHARACTERISTICS

The concept of the vacuum-photodiode detector is illustrated in Fig. 1. X rays impinge on a cathode in a vacuum, at angle ϕ. Many of them interact with atoms in the cathode via the photoelectric effect, ultimately transferring their energy to photoionized electrons, Auger electrons, and secondary electrons. Some of these electrons escape from the surface of the cathode, and if an anode is present and placed at an appropriate potential, the electrons will travel quickly to the anode and contribute to an electric current in external circuitry. Response to a given radiation field depends strongly on the materials and configuration used, detection efficiency depends largely on the fraction of primary and secondary electrons which are able to escape the cathode surface. There are two ways to optimize this.

One way is to choose a cathode material which has an electron range comparable to the stopping depth for x rays. For x rays above 10 keV, which could be crucial for imaging ITER (see Sec. IV), high-Z materials generally do a much better job of this than low-Z materials.

Another way is to choose a good geometry. Even for high-Z materials, the x-ray stopping depth is always considerably larger than the range of an electron at the same energy or below. We can overcome this problem by using a cathode that is not perpendicular to the incident x rays. For x rays which stop and generate electrons after passing through a path length of L in the cathode, the distance to the cathode surface is $L \sin \phi$ (see Fig. 1). By using a small value of ϕ, it should be possible to get more electrons per photon (a higher quantum yield) from a photocathode.

To investigate how this could work in practice, detailed numerical simulations were carried out to estimate quantum yield as a function of material and geometry, taking into account photoionized, Auger, and secondary electrons (using information from Refs. 4–8). Figure 2 shows calculated yields for aluminum ($Z=13$) and tungsten ($Z=74$) in the energy range of interest. Tungsten does far better than aluminum above 10 keV, and the quantum yield increases strongly at small angles (approximately as $1/\sin\phi$). The angle ϕ can be made quite small, but not arbitrarily so; below angles of about 1°, ''grazing-incidence'' reflection re-

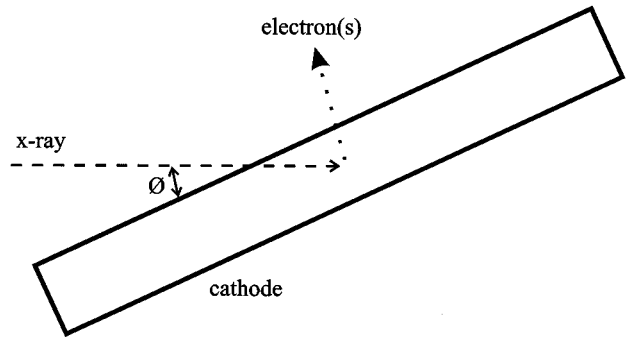

FIG. 1. Diagram of the cathode in a vacuum-photodiode x-ray detector.

duces the number of x rays that penetrate the cathode.

We conclude that a good approach for a detector that must have good efficiency for detecting x rays over the energy range 1–100 keV is to use a high-Z cathode oriented at a small angle to incident x rays. Most previous vacuum-photocathode detector designs have used low-Z cathodes with $\phi=90°$.

III. EXPERIMENTAL MEASUREMENTS

In order to verify that the above simulations will really lead us to the right choice of cathode material and geometry, a test detector was constructed. A 5×5 cm cathode was mounted on a rod of G10 which passes through an O-ring seal on a stainless-steel vacuum vessel; a knob on the rod end allows rotation of the cathode to any desired angle ϕ. The two cathodes tested are of tantalum ($Z=73$) and aluminum ($Z=13$) cleaned with solvent. The anode is a sheet of brass formed into a 7.5 cm ID cylinder whose axis corresponds to the rotation axis of the cathode (perpendicular to the page, in Fig. 1) and mounted inside the vacuum vessel on G10 standoff insulators. X rays enter through a 25-μm-thick polyimide window (nearly 100% transmitting for x rays of 5 keV and above), and then pass through an aperture in the cylindrical anode and hit the cathode. The chamber is connected to a roughing pump and a turbo pump via large-diameter flexible tubing.

Electronics consist of an adjustable-voltage bias supply, a simple, two-stage preamplifier adjusted to have appropriate gain (up to 5×10^7 V/A), and passband, and a digital oscilloscope.

Measurements of response to x rays were performed using a Norelco model 12045 x-ray source, which produces a 120 Hz output due to the use of a full-wave rectifier. Three different x-ray tubes were used in the source, with anodes made of chromium, copper, and molybdenum. It was possible to obtain nearly monochromatic x-ray spectra by filtering out most of the bremsstrahlung radiation from the three tubes with manganese, copper, and molybdenum foils, respectively, leaving well-defined K lines.[9]

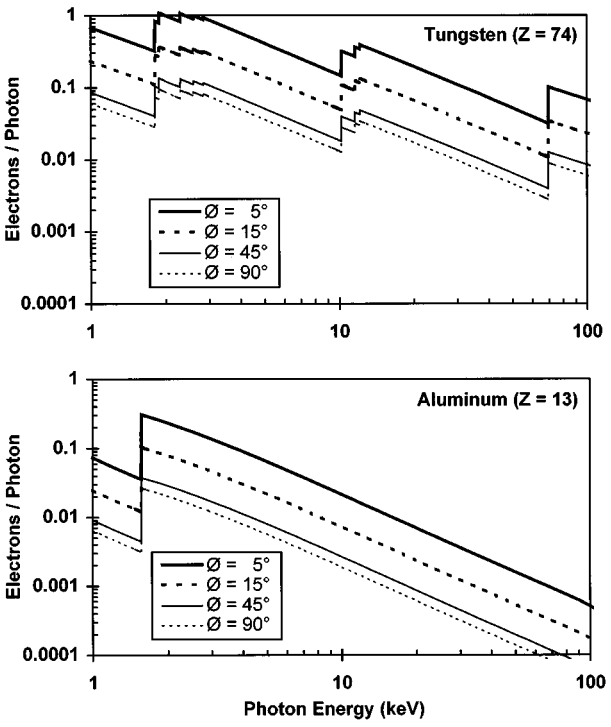

FIG. 2. Calculated photocathode quantum yield.

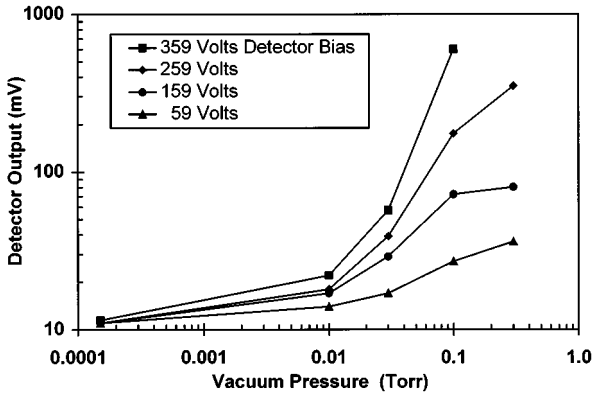

FIG. 3. Detector output vs bias voltage and vacuum pressure measured for a tantalum cathode at $\phi=90°$. The x-ray spectrum was from a copper-anode tube operated at 35 kV without any extra filtering.

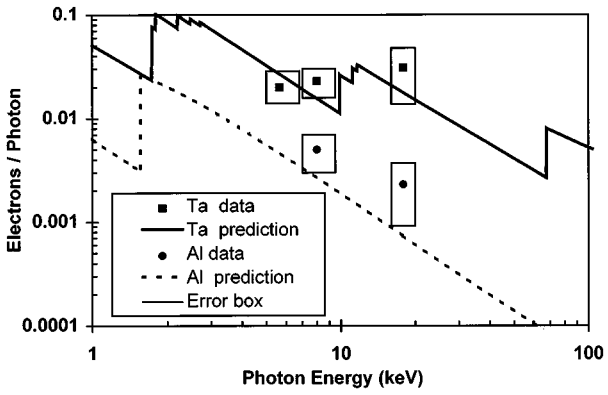

FIG. 4. Measured photocathode yields compared to predictions, for $\phi=90°$. The error-box heights are partly from detector measurement errors and mostly from uncertainties in the referenced SBD calibrations; the widths represent approximate widths of the x-ray spectra used for the measurements.

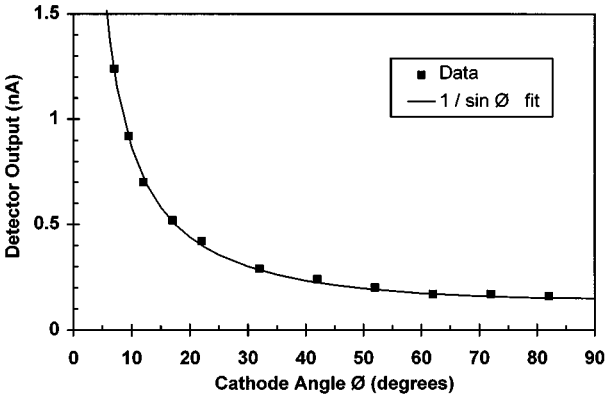

FIG. 5. Measured detector output vs cathode angle ϕ. A tantalum cathode was used, and the x-ray spectrum was from a copper-anode tube operated at 35 kV without any extra filtering. A small aperture over the detector window was used to make the x-ray beam small enough to allow for a wide variation in cathode angle (7°–90°) without a change in the solid angle of detection.

Detector response as a function of vacuum pressure and detector bias was measured for a tantalum cathode at $\phi=90°$, as shown in Fig. 3. A vacuum of order 10^{-4} Torr or better is required for pure photoelectric performance, but an interesting result is that extra detector efficiency can be obtained, if desired, by using a small amount of fill gas in the detector chamber. Amplification through avalanching in the gas is involved, and this phenomenon will be subjected to further study. Most of the following measurements were made with a detector bias of 100 V and a vacuum pressure of a few times 10^{-6} Torr.

Absolute detector efficiency at different x-ray energies was measured by comparing detector output with the output of a surface-barrier diode (SBD) of a type previously calibrated.[9] The results for a cathode angle of $\phi=90°$ are shown in Fig. 4, superposed on quantum-yield curves calculated as described in Sec. II. The measurements for the tantalum cathode agree very well with predictions. The measurements for aluminum are slightly high, but this could reflect the unknown purity of the sample or the presence of a surface oxide layer.

Detector response was also measured as a function of cathode angle ϕ (see Fig. 5) and x-ray tube current (see Fig. 6). Efficiency is essentially proportional to $1/\sin\varnothing$, as predicted, and the linearity of the detector response is excellent.

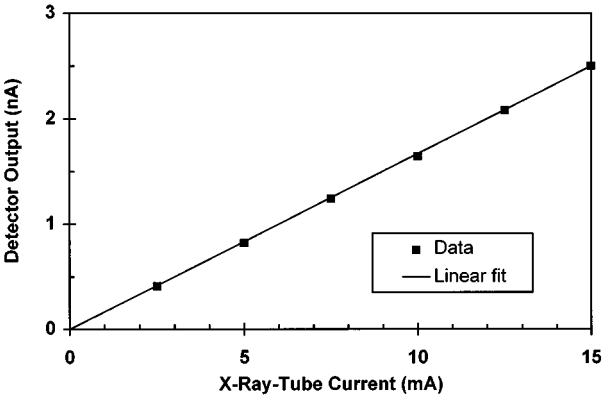

FIG. 6. Measurements of detector linearity, using an unfiltered copper-anode tube at 35 kV and a tantalum detector cathode at $\phi=12°$.

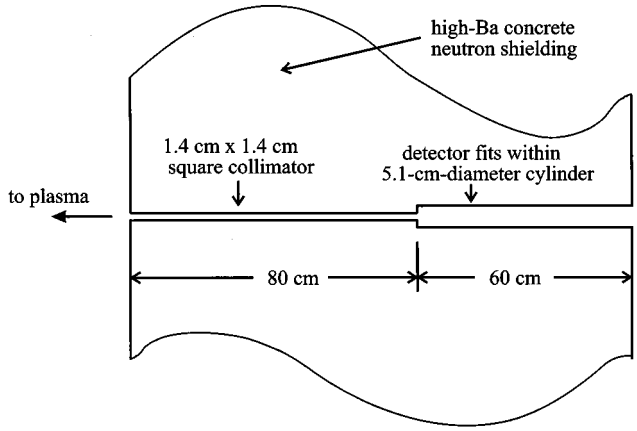

FIG. 7. Dimensions of the mount for each detector in the new JET x-ray imaging camera, based on specifications supplied by JET (see Ref. 10).

IV. A PROTOTYPE DESIGN

JET will be operating two series of D-T experiments over the next few years with 10 MW of fusion power. The JET diagnostic team has designed a new x-ray detector array[10,11] using solid-state detectors which are heavily shielded against stray neutrons and gamma rays (the total D-T operation time will be short enough that the detectors should not suffer fatal neutron-induced damage). We use their detector mount design (see Fig. 7) as a focus for detector design and theoretical evaluation with reference to a specific real-world application.

Figure 8 illustrates a detector prototype design for use in this mount. The cathode is made of a high-Z material such as tungsten or tantalum in order to provide good response to x rays above 10 keV. The cathode angle of $\phi=4°$ is designed to provide an increase by a factor of about 15 in quantum yield over that obtainable with a cathode normal to incoming

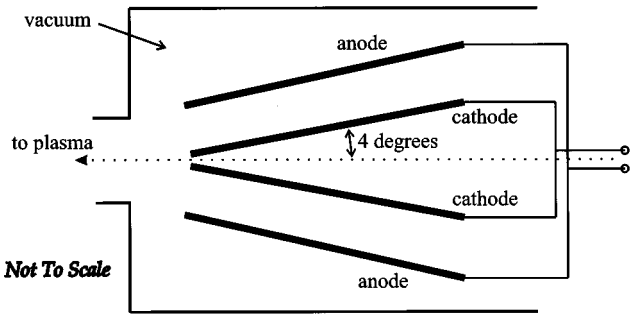

FIG. 8. A detector concept for the JET x-ray imaging camera mount shown in Fig. 7. The electrodes would be housed within a steel vacuum vessel, and a suitable window (such as 0.1 mm or more of Be) would separate the vacuum from the surrounding environment. The electrodes may be in the form of two pairs of flat plates, seen here edge on; or the cathode may be a conical surface surrounded by a cylindrically symmetric anode.

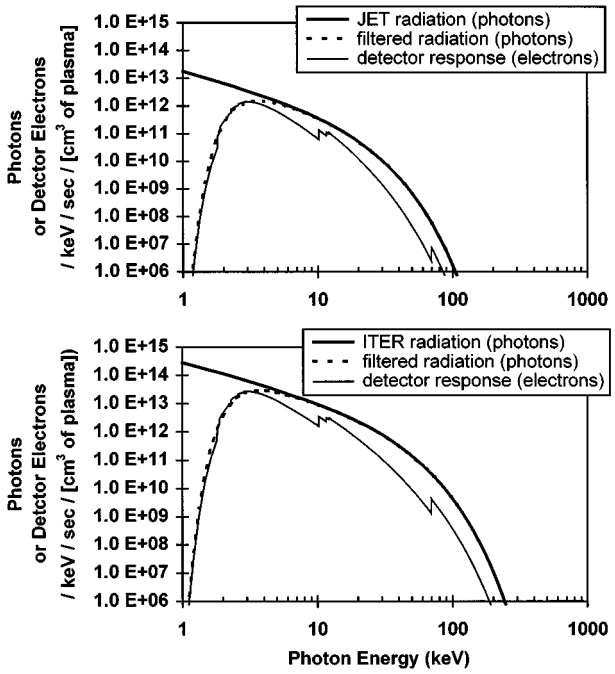

FIG. 9. Estimated continuum radiation spectra from the centers of the JET and ITER plasmas, and the response of the prototype detector design. The plasmas are assumed to have temperatures and densities as shown in Table I, with Z effective of 1.5, and a 0.25 mm Be window is assumed between plasma and detector. Detector response is given in terms of the number of electrons that would be generated if the detector could intercept all filtered x radiation from the plasma (imaging geometry is not included).

radiation. A steel housing will act as shielding, and the packaging and circuitry will be designed to minimize output currents due to reaction products of neutrons created in the detector structure. A low-noise, high-gain preamplifier using a special field-effect transistor (FET) input will be mounted in its own shielded container fixed directly to the back end of the detector chamber but offset to be out of the direct radiation field.

The geometry illustrated has a cathode–anode spacing of less than 1 cm. In combination with an appropriate bias voltage and good shielding, this should provide good immunity to external magnetic fields (which are expected[10] to be about 100 G in the JET camera). The close cathode–anode spacing also guarantees good intrinsic time response; with a detector bias of 1000 V, the electron transit time is about a nanosecond.

Figure 9 shows calculated estimates of continuum x-ray fluxes and spectra from the centers of the JET and ITER plasmas before and after filtering with a 0.25 mm berylium window (plasma parameters are from Refs. 10–12). Also shown is the result of folding the spectra into the calculated efficiency of the prototype detector design. If we want to study the plasma core by way of x-ray emissions, and if we can view the plasma through the equivalent of a 0.25 mm berylium window, then we're interested in the energy range from a few keV to a few tens of keV. With ITER, it is likely that thicker windows will be required and that only the radiation above 10 keV will be accessible; thus our emphasis on this part of the spectrum.

Using the specific detector geometry shown in Figs. 7 and 8 for JET, and the same arrangement scaled up proportionately in size for ITER, we predict the performance shown in Table I. The detector should provide good signal characteristics for JET and excellent performance on ITER.

TABLE I. Vacuum-photodiode performance estimates, assuming the detector and collimator geometries shown in Figs. 7 and 8 for JET and the same arrangement scaled in size for ITER. (Note that the tabulated detector output is approximately independent of the distance of the detector assembly from the plasma, as long as the collimator penumbra is substantially smaller than the minor radius. The plasma volume viewed goes as the distance squared, but the solid angle of the detector as seen from the plasma goes as the inverse of the distance squared.)

	JET	ITER
T_e (keV)	$10\,[1-(r/a)^2]^2$	$20\,[1-(r/a)^2]^2$
n_e (10^{14} cm^{-3})	$0.7\,[1-(r/a)^2]^{1/2}$	$1.4\,[1-(r/a)^2]^{1/2}$
Major radius R	3 m	8 m
Minor radius a	1 m	3 m
Detector output[a]	4 nA	2000 nA
Detector photon statistics noise[a,b]	0.4%	0.02%
Detector electronics noise[a,b]	0.02%	$<$1 bit of 16

[a]For a central line integral, assuming 0.25 mm Be filtering between plasma and detector.
[b]For 100 kHz sampling; noise will decrease if analog time constants are increased to appropriate values for lower sampling rates.

Finally, we note that while the vacuum photodiode should be essentially immune to radiation damage, silicon detectors in the same detector collimator arrangements assumed here would start to suffer radiation damage from a few thousand rads of neutrons within hours of operation on JET (10 MW fusion power) or minutes on ITER (1000 MW fusion power).

ACKNOWLEDGMENT

This work was supported in part by U.S DOE Grant No. DE-FG02-95-ER81934. We gratefully acknowledge useful conversations with R. Gill, A. Edwards, and B. Alper of JET; A. Costley of ITER; and K. Wenzel of MIT. In addition, we thank I. Olmez of MIT for the loan of x-ray tubes.

[1] A. T. Ramsey, Rev. Sci. Instrum. **66,** 871 (1995).
[2] P. Lee, J. Gernhardt, C. J. Armentrout, and R. T. Snider, Rev. Sci. Instrum. **59,** 883 (1988).
[3] S. J. Zweben, C. R. Menyuk, and R. J. Taylor, Rev. Sci. Instrum. **50,** 972 (1979).
[4] W. H. McMaster, N. Kerr Del Grande, H. H. Mallett, and H. H. Hubbell, Lawrence Radiation Laboratory Report No. UCRL-50174 Sec. II Rev. 1, 1969 (unpublished).
[5] B. L. Henke, J. P. Knauer, and K. Premaratne, J. Appl. Phys. **52,** 1509 (1981).
[6] T. Tabata, R. Ito, and S. Okabe, Nucl. Instrum. Methods **103,** 85 (1972).
[7] W. Bambynek, B. Crasemann, R. W. Fink, H. U. Freund, H. Mark, C. D. Swift, R. E. Price, and P. V. Rao, Rev. Mod. Phys. **44,** 716 (1972).
[8] A. S. Ganeev and I. M. Izrailev, Sov. Phys. Tech. Phys. **31,** 270 (1961).
[9] K. W. Wenzel and R. D. Petrasso, Rev. Sci. Instrum. **59,** 1380 (1988).
[10] R. D. Gill (private communications).
[11] B. Alper, S. Dillon, A. W. Edwards, R. D. Gill, R. Robins, and D. J. Wilson, Rev. Sci. Instrum., these proceedings.
[12] A. E. Costley *et al.*, Bull. Am. Phys. Soc. **39,** 1594 (1994).